

Viscoelasticity and rheological hysteresis

Shweta Sharma,¹ V. Shankar,^{1, a)} and Yogesh M. Joshi^{1, b)}

*Department of Chemical Engineering, Indian Institute of Technology Kanpur,
Kanpur 208016, India*

(Dated: 3 March 2022)

Rheological characterization of complex fluids subjected to cyclic shear-rate sweep often exhibits hysteresis. Since both viscoelastic and thixotropic materials show hysteresis loops, it is important to understand distinguishing features (if any) in the same shown by either. Lately, there has been substantial work that attempts to relate the area enclosed by the hysteresis loop with the manner in which shear rate is varied in the cycle, in order to infer thixotropic parameters of a material. In this work, we study the Giesekus model, which is a standard non-linear viscoelastic model, under application of cyclic shear-rate sweep. We find that this model produces each type of hysteresis loop that has hitherto been ascribed to thixotropic materials. We also show that the area of the hysteresis loop for a viscoelastic material as a function of sweep rate shows bell-shaped/bi-modal curves as also observed for the thixotropic materials. This study illustrates that caution needs to be exercised before attributing hysteresis loops and associated features observed in a material exclusively to thixotropy. Another feature related to the hysteresis loop is the occurrence of shear banding instability. We find that viscoelastic hysteresis may not have any connection to shear banding instability.

^{a)}Electronic mail: vshankar@iitk.ac.in

^{b)}Electronic mail: joshi@iitk.ac.in

I. INTRODUCTION

Viscoelasticity concerns ability of a material to store elastic potential energy upon application of deformation field over timescales comparable to observation timescale. Correspondingly the time over which the stress relaxes is termed as relaxation time of a material. When a viscoelastic material is subjected to cyclic down-up (or up-down) shear rate ramp, either step wise or continuous, the transient stress induced in the material depends on the nature of a material, the deformation history, the value of instantaneous shear rate, and the step time (or the ramp rate). Consequently, depending upon specifics of the given (or chosen) material and the flow field, stress in a material at given shear rate in a forward path may differ from that associated with the reverse path leading to hysteresis. In the literature, the subject of hysteresis in viscoelastic materials has been studied in detail both experimentally and theoretically. On an independent but related note, it has been well established that thixotropy, which concerns increase in viscosity under no flow or weak flow conditions and decrease in viscosity under strong flow conditions, shows many behavioural similarities with viscoelasticity [1–4]. In particular, thixotropic materials also show hysteresis in cyclic shear rate sweep experiment. In the literature, certain features of hysteresis loop have been identified as discriminating signatures of the presence of thixotropy in a material. Specifically, the area enclosed by a hysteresis loop as a function of step time in a stepwise down-up ramp has been proposed to show some unique features for a thixotropic material. In our earlier study [4], we assessed four different experimental protocols that have been proposed to distinguish thixotropy and viscoelasticity. We found that stress relaxation and/or creep experiments at different waiting times lead to unique signatures for thixotropic vis-a-vis viscoelastic materials. In this work, we theoretically assess the hysteresis loop method by employing a standard nonlinear viscoelastic model and study to what extent a viscoelastic material demonstrates features of hysteresis considered to be unique for thixotropic materials and implications of the same.

Hysteresis in viscoelastic materials is observed because of the finite time required by the materials to reach the steady state corresponding to the applied flow field which is governed by the magnitude of their relaxation time. Consequently, if the sweep rate is faster than the relaxation time of the material then due to incomplete relaxation of stress during down-sweep and incomplete buildup of stress during up-sweep, shear stress does not trace the same path in the down-sweep and up-sweep flow. Moreover, if the applied shear rate is in the non-linear region, then the hysteresis loop area increases due to presence of stress undershoot during down-sweep and stress overshoot

during up-sweep shear flow. Viscoelastic hysteresis has been discussed in detail by Bird and Marsh [5] and Marsh [6] using the viscoelastic model developed by Bird and Carreau [7]. They studied shear rate ramp flows with and without slow varying flows assumption ($De < 1$). Marsh [6] proposed various kinds of viscoelastic hysteresis loops using the Bird-Carreau model that are redrawn and shown in Fig. 1. In this figure, shear stress is plotted as a function of shear rate for different values of total time of experiment. Figure 1(a) shows loops that can be obtained using either triangular shear rate ramp up and ramp down flow or sinusoidal shear rate ramp up and ramp down. Figure 1(b) shows loops that can be obtained using shifted sinusoidal shear rate ramp up and ramp down. The type 1-9 curves in Fig. 1(a) and type 1-3, 7-9 curves in Fig. 1(b) are shown in the decreasing order of the value of total experiment time. The total experiment time is maximum for type 1 and it is minimum for type 9 (in Fig. 1(a)) and type 10 (in Fig. 1(b)) curves. The type 1 and 2 loops in Fig. 1(a) can be obtained for the case in which the the sweep rate is much greater than inverse of characteristic relaxation time of the fluid. The maximum shear rate for the type 1 loop is in the linear region and for the type 2 curve, the maximum shear rate is in the non-linear region. The type 3-9 loops can be obtained by varying the total experiment time in decreasing order. In these type of loops, it is shown that as the value of ramp time decreases, the area of hysteresis loop increases. The humps in these loops during up-sweep flow can be obtained due to stress overshoot and non-zero stress can be obtained at zero shear rate due to incomplete stress relaxation. The type 1-3 hysteresis loops in Fig. 1(b) for the case of shifted sinusoidal wave shear rate sweep flow are similar to loops presented in Fig. 1(a). Type 7 loop shows that the hump in the loop is not as pronounced as type 6 loop in Fig. 1(a). Type 10 hysteresis loop shown in Fig. 1(b) can be obtained using a viscoelastic material in a shifted sinusoidal shear rate ramp up and ramp down flow field. Hysteresis loops obtained due to linear and non linear viscoelastic effects have also been explored in the literature [8 and 9] using Wagner model and Maxwell model. Thixotropic materials are inherently out of thermodynamic equilibrium even in the stress free state, and therefore undergo time dependent evolution of microstructure under quiescent conditions in order to attain the low energy states. As a result viscosity of such material continuously increases as a function of time. The microstructure developed in these materials, in principle, can be reversed or gradually broken down upon the application of deformation field of sufficiently high magnitude, which causes time dependent decrease in viscosity. During a shear rate sweep experiments performed on such materials, the microstructure breaks down at high shear rates and as shear rate is decreased sequentially, it again starts to buildup. Furthermore, as shear rate is increased during the up-sweep shear flow,

the developed microstructure requires more stress than during the down-sweep shear flow for the same value of shear rate. Therefore, shear stress does not trace the same path during the down-sweep and up-sweep shear flow for a thixotropic material. More detailed discussion on thixotropy, and hysteresis due to thixotropy is presented in the state of the art review articles [1–3, 10–12].

Hysteresis in complex fluids was first observed in paints by McMillen in 1932 [13]. Since this study, many thixotropic and non-thixotropic complex materials in the literature has been reported to show hysteresis. Some of these materials are mineral oil [14 and 15], lithographic ink [16], waxy potato starch [17], cellulose nanocrystal suspensions [18], mud and cement pastes [19–21], sodium alginate solutions [22], solder and adhesive pastes [23], ferrofluids [24], sodium carboxymethyl-cellulose hydrogels [25], fluorinated guar gums [26], Carbopol microgels [27], microfibrillar cellulose water dispersions [28], sodium polyacrylate Laponite solution [29], polystyrene solutions [30], waxy crude oil [31], acrylic emulsion paints [32], pulp fibre suspensions [33], colloidal star gels [34], foams and emulsions [35], Ludox gels [36], etc. This list contains both non-thixotropic viscoelastic materials as well as thixotropic materials. Interestingly, the qualitative nature of the hysteresis loops observed in above mentioned materials, including those that are labelled as thixotropic, are similar to the hysteresis loops shown in Figure 1(b) obtained by Marsh [6] specifically for non-aging viscoelastic materials. It is therefore, imperative to detect characteristic features of hysteresis loops that distinguish viscoelasticity from thixotropy. Mewis [11], Barnes [1], and Mewis and Wagner [2] considered hysteresis loop as a quick way to measure thixotropy in a material and mentioned it as an useful method for industrial use. However, these review articles also pointed out that hysteresis loop experiment is affected by both time and shear rate, and consequently, it is not an ideal way to identify a material as thixotropic. In these papers, the authors also sound a note of caution that hysteresis loops are common to both thixotropic and viscoelastic materials but also mentioned that viscoelastic hysteresis might only be observed when the sweep rates are sufficiently high. Although, such cautionary advice in the literature is particularly focused on the viscoelastic materials that have a low relaxation time, very high relaxation time non-thixotropic viscoelastic materials may show hysteresis loops at sweep rates that are not sufficiently high (such sweep rates are commonly used in experiments to obtain flow curves as mentioned below).

In the recent years, hysteresis in thixotropic and simple yield stress materials has been studied extensively. Divoux et al. [37] experimentally studied rheological hysteresis using Laponite, carbon black, Mayonnaise, and Carbopol microgel. They performed shear rate down sweep fol-

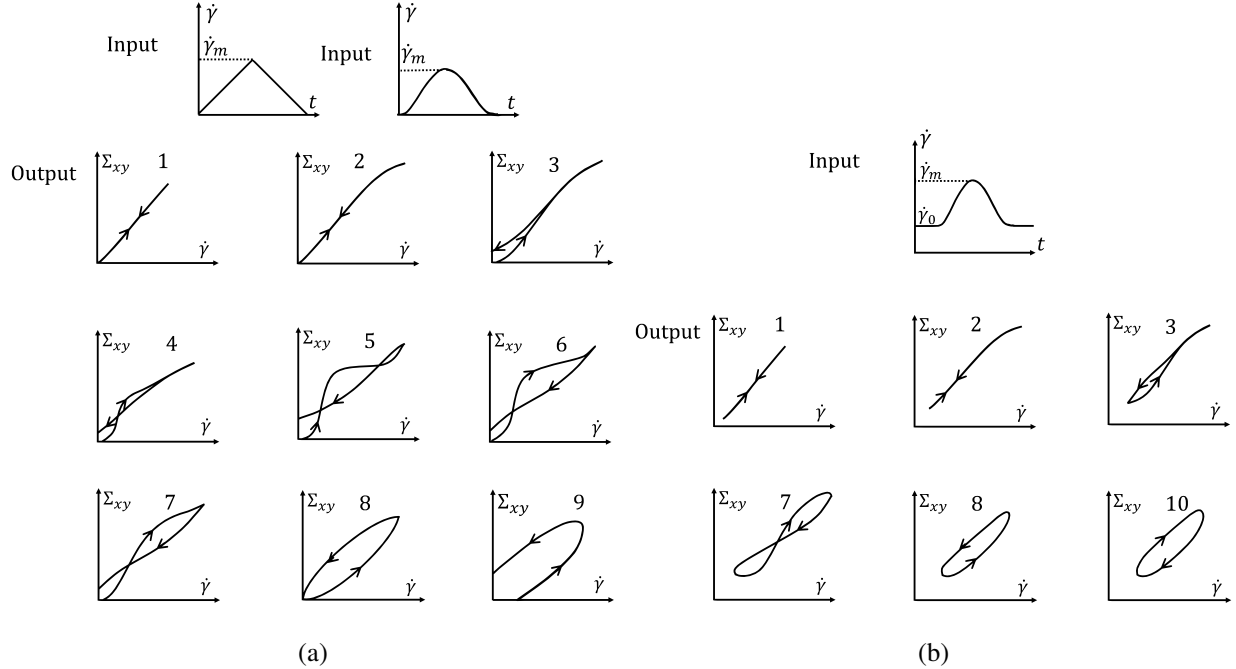


FIG. 1. Different types of hysteresis loops proposed by Marsh [6] for a given input deformation flow field are shown in this figure. These loops can be obtained using a viscoelastic material for (a) triangular shear rate ramp up and ramp down flow or sinusoidal shear rate ramp up and ramp down, with a maximum shear rate, $\dot{\gamma}_m$ and (b) shifted sinusoidal shear rate ramp up and ramp down, presheared at $\dot{\gamma}_0$. These schematics are due to B. Duane Marsh, *Transactions of the Society of Rheology* 12:4, 489-510 (1968).

lowed by a shear rate up sweep experiment using all four samples and calculated the area of the resulting hysteresis loop. They also calculated the area of loop obtained due to inhomogeneity in the velocity profile during the shear rate sweep experiments. The area of hysteresis loop and area of inhomogeneous velocity profiles as a function of sweep time was found to show a bell shaped curve for Laponite and carbon black solution. The area of both loops showed a continuing decrease with sweep time for Mayonnaise and Carbopol microgel solutions. Divoux et al. concluded that the value of sweep time at which a maximum loop area is observed to be related to the characteristic timescale of the material, which was later termed as thixotropic timescale of the material [38]. The absence of peak in Carbopol and Mayonnaise was attributed to a negligible value (or of a significantly smaller order of magnitude) of thixotropic timescale.

Divoux et al. [37] also showed results of the local velocity profile corresponding to the shear rate sweep experiments and found that hysteresis in these materials is interlinked with shear banding which was suggested to be triggered due to stress overshoot. The authors also prescribe a

specific experimental protocol to study hysteresis. The suggested protocol is to first preshear the material at a very high shear rate so as to remove any prior history. After preshear, the next step is down-sweep from a very high shear rate to a very small value of shear rate and the shearing period (δt) at each shear rate is fixed. The number of shear rates in each decade (n) are also fixed. This protocol has been followed in most of the studies following the article by Divoux et al. [37]. Puisto et. al. [39] studied a simple yield stress model using a homogeneous and a cylindrical geometry, and showed that these materials are also capable of showing a bell shaped curve. They also found that hysteresis and shear banding may not always be related in such fluids. Radhakrishnan et al. [40] studied rheological hysteresis in detail using simple fluidity model and the soft glassy rheology (SGR) model [41 and 42] to understand hysteresis in simple yield stress and viscosity bifurcating fluids. They compared their results with the experimental results of Divoux et al. [37] and found a good agreement between experimental and simulation results. Radhakrishnan et al. also emphasised on getting a closed hysteresis loop in simulation results so that these results can be compared with experiments. The authors attributed the lack of closed hysteresis loop to be the reason for getting a bell shaped curve for simple yield stress fluids by Puisto et al.[39]. Jamali et al. [43] studied hysteresis in soft glassy materials for three different lengthscale of material's structure- microscopic, mesoscopic and macroscopic scale. The authors employed dissipative particle dynamics and concluded that the soft glassy materials show hysteresis on all the three different scales. The plot of area of all the hysteresis loops with sweep time normalised by the characteristic timescale at each scale showed a bell-shaped master curve. This result is also in agreement with the results of Divoux et al. [37] and Radhakrishnan et al. [40].

The motivation of the present study is as follows. Real materials that have been studied in the literature and termed as thixotropic are also usually viscoelastic. In this context, an important question that arises is as follows - is it possible to identify a completely unknown material if it is viscoelastic or thixotropic on the basis of hysteresis loop? Larson [10] in his seminal review noted that viscoelastic time scales range from nanoseconds to centuries. Bird and Marsh [5] and Marsh [6] have already addressed this question, albeit partially, by clearly showing the various possible hysteresis loops in viscoelastic materials. In this study, we show that viscoelastic hysteresis loops proposed by Marsh [6] using a flow protocol of continuous ramp up and down shear flow can be obtained only for a low relaxation time viscoelastic material. If the relaxation time of viscoelastic materials is sufficiently high, then the type of hysteresis loops that can be observed will not remain same as of low relaxation time viscoelastic materials. In addition, more recently, the peculiar

features of area of hysteresis loop as a function of sweep time (as discussed above) have also been reported for thixotropic materials. Therefore, an important question that remains to be addressed is what kind of signature viscoelastic materials would demonstrate for the protocol suggested by Divoux et al. [37], wherein they reported a bell shaped curve for the area of hysteresis loop when plotted against sweep time. To this end, in this work, we study the non-linear viscoelastic Giesekus model for a proposed protocol and analyse the obtained shear stress-strain rate hysteresis loops and compare these with the hysteresis loops obtained in literature for viscosity bifurcating, simple yield stress and other viscoelastic materials and models.

The rest of this paper is organised as follows: we discuss the flow protocol, Giesekus model and the governing equations in section II. We then discuss hysteresis in low and high relaxation time viscoelastic materials. Subsequently, we present features associated with area of viscoelastic hysteresis loops followed by a detailed analysis of the observed behavior in section III. Finally, in section III, we discuss viscoelastic hysteresis in relation to shear banding. The important conclusions of this study are discussed in section IV.

II. MODEL AND GOVERNING EQUATIONS

In this work, we study shear rate sweep flow of a model viscoelastic fluid between two parallel plates. The plates are separated by a distance H in the y^* direction and are assumed to be of infinite length in x^* and z^* directions. We apply shear rate sweep in both increasing and decreasing order. For shearing the fluid at a fixed shear rate, we assume that both the plates are initially ($t^* = 0$) at rest and we shear the fluid by moving the top plate with a constant velocity U in x^* direction. In this case, the continuity equation (mass balance) gets satisfied by itself $\nabla \cdot \tilde{u}^* = 0$, where \tilde{u}^* is the velocity vector. We assume the shear flow to be inertialess and consequently, the simplified Cauchy momentum equation can be expressed as follows:

$$\nabla \cdot \tilde{\Sigma}^* = 0, \quad (1)$$

where, $\tilde{\Sigma}^*$ is the total stress tensor. We also consider the total stress to be a summation of viscoelastic stress (polymer contribution, $\tilde{\sigma}^*$) and a Newtonian stress (solvent contribution) which can also accommodate the faster relaxing modes in a polymeric solution.

$$\underset{\approx}{\Sigma^*} = \underset{\approx}{\sigma^*} + \mu_s \underset{\approx}{\dot{\gamma}^*}, \quad (2)$$

where, μ_s is the viscosity of solvent in the polymeric solution and $\underset{\approx}{\dot{\gamma}^*} = (\nabla u^* + (\nabla u^*)^T)$, is the rate of strain tensor.

The viscoelastic contribution to the total stress is governed by $\underset{\approx}{\sigma^*}$ according to the Giesekus model [44]. The dimensional form of constitutive model is expressed as:

$$\underset{\approx}{\sigma^*} + \tau \underset{\approx}{\sigma^*} = -\alpha \frac{\tau}{\mu_p} (\underset{\approx}{\sigma^*} \cdot \underset{\approx}{\sigma^*}) + \mu_p \underset{\approx}{\dot{\gamma}^*}, \quad (3)$$

where, α is the dimensionless mobility factor that accounts for anisotropic hydrodynamic drag on polymeric molecules and μ_p is the polymeric contribution to the zero shear viscosity. This model is a non-linear phenomenological model, which has been successful in predicting transient and steady state flow behaviour of polymeric and wormlike micellar solutions [45–47]. The advantage of using Giesekus model over Oldroyd-B model is its ability to fit the shear thinning as well as first and second normal stress differences obtained in the experimental results of polymeric solution due to the presence of quadratic stress term.

We non-dimensionalize the length scale by gap width (H), velocity by top plate velocity (U) and time scale by longest relaxation time of the polymeric solution (τ). We non-dimensionalize all the stress components by $\left(\frac{\mu_s + \mu_p}{\tau}\right)$. We represent dimensional terms with $*$ superscript. The dimensionless numbers used in this study are the Weissenberg number $Wi = \frac{\tau U}{H}$ and the ratio of solvent viscosity to zero shear viscosity of the polymeric solution $\eta_s = \frac{\mu_s}{\mu_s + \mu_p}$. In this study, we obtain all the results using $\alpha = 0.1$. We also use $\alpha = 0.2$ and 0.3 , and observe results to be qualitatively similar suggesting the results are not sensitive to value of α . The component-wise equations of Giesekus model in non-dimensional form for simple shear flow can be expressed as follows:

$$\frac{\partial \sigma_{xy}}{\partial t} = -\frac{\alpha}{(1 - \eta_s)} (\sigma_{xx} + \sigma_{yy}) \sigma_{xy} + [(1 - \eta_s) + \sigma_{yy}] Wi \dot{\gamma} - \sigma_{xy}, \quad (4)$$

$$\frac{\partial \sigma_{xx}}{\partial t} = -\frac{\alpha}{(1 - \eta_s)} (\sigma_{xx}^2 + \sigma_{xy}^2) + 2Wi \dot{\gamma} \sigma_{xy} - \sigma_{xx}, \quad (5)$$

and

$$\frac{\partial \sigma_{yy}}{\partial t} = -\frac{\alpha}{(1 - \eta_s)} (\sigma_{yy}^2 + \sigma_{xy}^2) - \sigma_{yy}. \quad (6)$$

Flow protocol: We follow the flow protocol that is suggested by Divoux et al. [37] to study hysteresis. According to this flow protocol, we pre-shear, wherein we subject the model to high shear rate which is same as the maximum shear rate. For shear rate sweep experiments, shear rate is first decreased in steps with the system allowed to be in a given shear rate for a time δt for each step. After reaching the minimum value of shear rate, it is again increased to the maximum value in steps and δt time on each step. The time δt is also referred to as sweep rate [37] or shearing time [43] in the literature. We measure the area of hysteresis loop as suggested by Divoux et al [37] which is expressed as follows:

$$A_\sigma = \int_{Wi_{\min}}^{Wi_{\max}} |\Delta\Sigma_{xy}(Wi)| d\log Wi \quad (7)$$

where, $|\Delta\Sigma_{xy}(Wi)| = |\Sigma_{xy,down}(Wi) - \Sigma_{xy,up}(Wi)|$. We also measure area under the down-sweep $\Sigma_{xy} - Wi$ curve as follows:

$$A_d = \int_{Wi_{\min}}^{Wi_{\max}} \Sigma_{xy}^d(Wi) d\log Wi \quad (8)$$

where, $\Sigma_{xy}^d(Wi)$ is the stress as a function of Wi during down-sweep shear flow. The Wi values are equally spaced on the logarithmic scale to avoid dominance of higher shear rate values. The number of steps per decade are fixed and is represented by n . As we consider inertialess flow and a planar geometry, the shear stress is assumed to be constant in the y direction. We solve the above equations (Eqs. 4-6) for down-sweep and up-sweep shear flow using the ode45 subroutine by MATLAB®.

III. RESULTS AND DISCUSSION

We present results for the down-sweep and up-sweep by plotting shear stress as a function of Wi , in which shear stress value is obtained at the end of δt time spent at each shear rate step. Furthermore, we study down-sweep and up-sweep flow of two categories of viscoelastic materials: (i) the materials with relaxation time of the order of 10^{-1} s, and (ii) the materials with relaxation time of the order of 10^6 s or higher. We also investigate the possibility of hysteresis loop in these viscoelastic materials and resemblance with the hysteresis loops observed for thixotropic fluids in the literature.

A. Low relaxation time viscoelastic materials

Consider a non-thixotropic viscoelastic material with a relaxation time (τ) of the order of 10^{-1} s. The lowest value of shear rate generally attainable in a standard rheometer is 10^{-3} s $^{-1}$ while the higher value of shear rate that is attainable is 10^3 s $^{-1}$. We study a case of viscoelastic material that has a relaxation time, $\tau = 10^{-1}$ s. In this case, the range of the value of Wi for down-sweep and up-sweep experiments is $10^{-4} - 10^2$ if shear rate is varying from $10^{-3} - 10^3$ s $^{-1}$. We study down-sweep and up-sweep flow for different values of δt varying from 10^{-6} to 10^2 . To obtain the results presented below, we first decrease the shear rate (down-sweep) in a step-wise manner to attain a minimum value (from $Wi = 10^2$ to $Wi = 10^{-4}$). After reaching the minimum shear rate, we increase the shear rate (up-sweep) to the initial maximum shear rate value (i.e., from $Wi = 10^{-4}$ to $Wi = 10^2$) in a step-wise manner. Figure 2 shows shear stress as a function of Wi for different values of δt and Wi is varying from 10^{-4} to 10^2 . As mentioned above, shear stress value is obtained at the end of δt time at each step. We also show the corresponding shear stress and Wi evolution as a function of time that is normalised with δt in Fig. S1 presented in the supplementary material.

Cyclic down-up sweep shear flow using Giesekus model at different values of δt results in hysteresis loops as down-up sweep stress does not coincide for some values of δt as shown in Fig. 2. It can be seen that there are four types of hysteresis loops that can be obtained using a viscoelastic material of relaxation time of the order of 10^{-1} s. All four types of hysteresis loops show decrease in stress during down-sweep (decrease in shear rate). During up-sweep (increase in shear rate), stress first decreases and then increases. This feature is clearly visible in Figs. 2 and S1. In Fig. 2(a), hysteresis loop comprises of a closed loop in which there is a minimal change in stress over the cyclic shear rate sweep. This minimal change in stress is also clearly depicted in stress versus time plot in Fig. S1(a) in the supplementary material. We term these kind of loops as type 1. Figures 2(b)-2(e) shows loops that has a relatively higher change in stress in cyclic shear rate sweep. These loops are termed as type 2. The loops can be open (Fig. 2(b)-2(d)) for lower values of δt and closed (Fig. 2(e)) for higher values of δt . Figures 2(f)-2(j) depicts loops that have one crossover of down-up sweep stress because of stress overshoot observed at higher values of Wi in up-sweep. These loops can be categorised as type 3. Stress overshoot is clearly visible in Fig. S1(f)-S1(j) in supplementary material. Type 3 loops are also can be open (Fig. 2(f)-2(g)) for lower values of δt and closed (Figs.2(h)-2(j)) for higher values of δt . Figure 2(k) shows a loop in which

there is no crossover of down-up sweep stress and the loop is closed. Such loops can be labelled as type 4. This type of loop gets formed because of difference in down-sweep and up-sweep stress only for lower values of Wi . For higher values of Wi , down-up stress overlaps each other. For $\delta t = 10^2$, down-up sweep stress completely overlaps each other resulting in absence of hysteresis loop as shown in Fig. 2(l).

The down-sweep stress always shows decrease in the type 1-4 hysteresis loops while up-sweep stress always shows first decrease and then increase. The decrease in down-sweep stress in type 1-4 hysteresis loop is to attain its steady state value corresponding to Wi in the given δt time at each step. If the value of stress at the end of down-sweep flow is higher than its steady state value then up-sweep stress will first show decrease. The increasing part of up-sweep stress is due to early elastic effects in high Wi region driving stress away from the steady state values at each Wi . This stress response is governed by the initial value of $\tilde{d\Sigma}/dt$ which depends on the value of Wi of previous step as also stated in literature [48–50]. Type 1, 2 and 4 hysteresis loops can be obtained by linear viscoelasticity, while type 3 hysteresis loop can only be obtained by a non-linear viscoelastic model.

These hysteresis loops resulting because of competition between finite time required for stress to reach respective steady state values during down-sweep and up-sweep shear flow and the time scale of experiment, δt are in agreement with the results of Bird and Marsh [7] and Marsh [6]. The open hysteresis loops observed at low values of δt (Figs. 2(a)-2(d)) without any crossover are also similar to hysteresis loops observed for simple yield stress fluids by Puisto et. al. [39].

B. High relaxation time viscoelastic materials

In this subsection, we consider the case of a viscoelastic material that has relaxation time of the order of 10^6 s (≈ 11.5 days) or higher. We study cyclic shear rate down-up sweep of such materials using the Giesekus model by first varying Wi from 10^9 to 10^3 (down-sweep) in a step-wise manner. Secondly, we increase Wi from 10^3 to 10^9 (up-sweep) in a step-wise manner. As mentioned above, this range of Wi is also in accordance with the range of shear rate values that are generally attainable in standard rheometer to obtain the flow curve of a material. In this case, we also consider η_s is 10^{-7} to magnify viscoelastic effects that can be observed at high value of Wi .

Figure 3 show results for down-sweep and up-sweep shear flow using Giesekus model for different values of δt . We also show the corresponding shear stress and Wi evolution as a function

of time that is normalised with δt in Fig. S2 in supplementary material. In this case, there can be three types of hysteresis loops that can be obtained using a high relaxation time viscoelastic material. In all these hysteresis loops, down-sweep (decrease in Wi) stress always shows decrease while the behaviour of up-sweep (increase in Wi) stress is different in each type of loop. Figures 3(a)-3(c) shows hysteresis loops in which down-sweep stress is always above the up-sweep stress. These hysteresis loops can be termed as type 5. This type 5 category loop is similar to type 2 closed hysteresis loop of low relaxation time viscoelastic materials. The up-sweep stress in type 1 hysteresis loop show a decrease and then increase for the same reason as noted in the case of low relaxation time viscoelastic material. Hysteresis loops shown in Figs. 3(d)-3(f) are labelled as type 6. These loops show a crossover of down-sweep and up-sweep stress. The up-sweep stress first show decrease and then increase that is also accompanied with an overshoot. Hysteresis loops depicted in in Figs. 3(g)-3(l) are termed as type 7. These loops show up-sweep stress always above the down-sweep stress.

Interestingly, stress at the end of down-sweep first decreases (with increase in δt) and then increases to finally attain its steady state for $\delta t = 1$. This is in contrast to a gradual decrease of stress at the end of down-sweep to attain its steady state value for low relaxation time viscoelastic materials (Fig. 2). This is due to the stress undershoots in the shear thinning region (least steeper region of constitutive curve). These stress undershoots are clearly visible in Fig. S2 in supplementary material. Similarly, stress overshoot in the shear thinning region in the up-sweep leads to type 7 hysteresis loops in which only stress overshoot lead to difference in down and up sweep stress. The stress overshoot in the up-sweep shear is also visible in Fig. S2 in supplementary material. We also observe that the value of stress remains same (at steady state) for high shear rate branch in all the hysteresis loops. This is due to the fact that in this region viscosity remains constant with shear rate, and hence no undershoot and overshoot in stress is present (as also shown in Fig. S2 in supplementary material). Also, at such high shear rates, the initial rate of change of stress is significantly high. Therefore, even if $\delta t = 10^{-8}$, stress immediately reaches steady state at each step during down-sweep and up-sweep. This effect always leads to a closed hysteresis loop as compared to open hysteresis loop obtained in case of low relaxation time viscoelastic materials shown in Fig. 2. The closed hysteresis loops show resemblance to generally observed loops experimentally for thixotropic materials. The hysteresis loops observed for high relaxation time materials also show a particular kind of loop in which stress during up-sweep shear flow is only higher and not lower than stress during down-sweep shear flow in the region of loop formation (Figs. 3(g)-

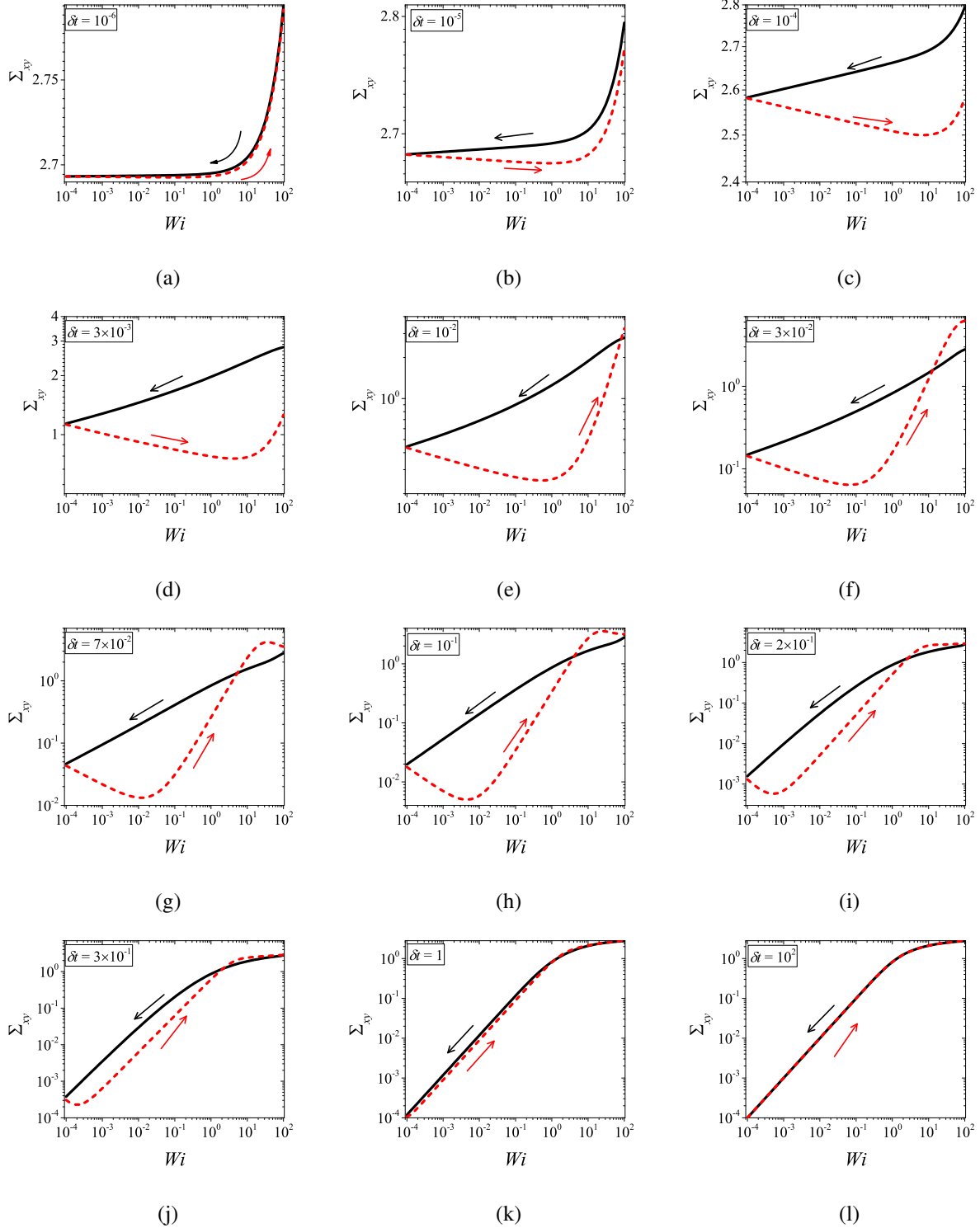


FIG. 2. Types of hysteresis loops (in a down-up shear rate cycle) obtained for the low relaxation time viscoelastic material using different values of δt and $\eta_s = 10^{-3}$. Shear stress is plotted as a function of Wi for δt equals to (a) 10^{-6} , (b) 10^{-5} , (c) 10^{-4} , (d) 3×10^{-3} , (e) 10^{-2} , (f) 3×10^{-2} , (g) 7×10^{-2} , (h) 10^{-1} , (i) 2×10^{-1} , (j) 3×10^{-1} , (k) 1, and (l) 10^2 . Solid lines shows down-sweep and dashed line shows the up-sweep shear flow results.

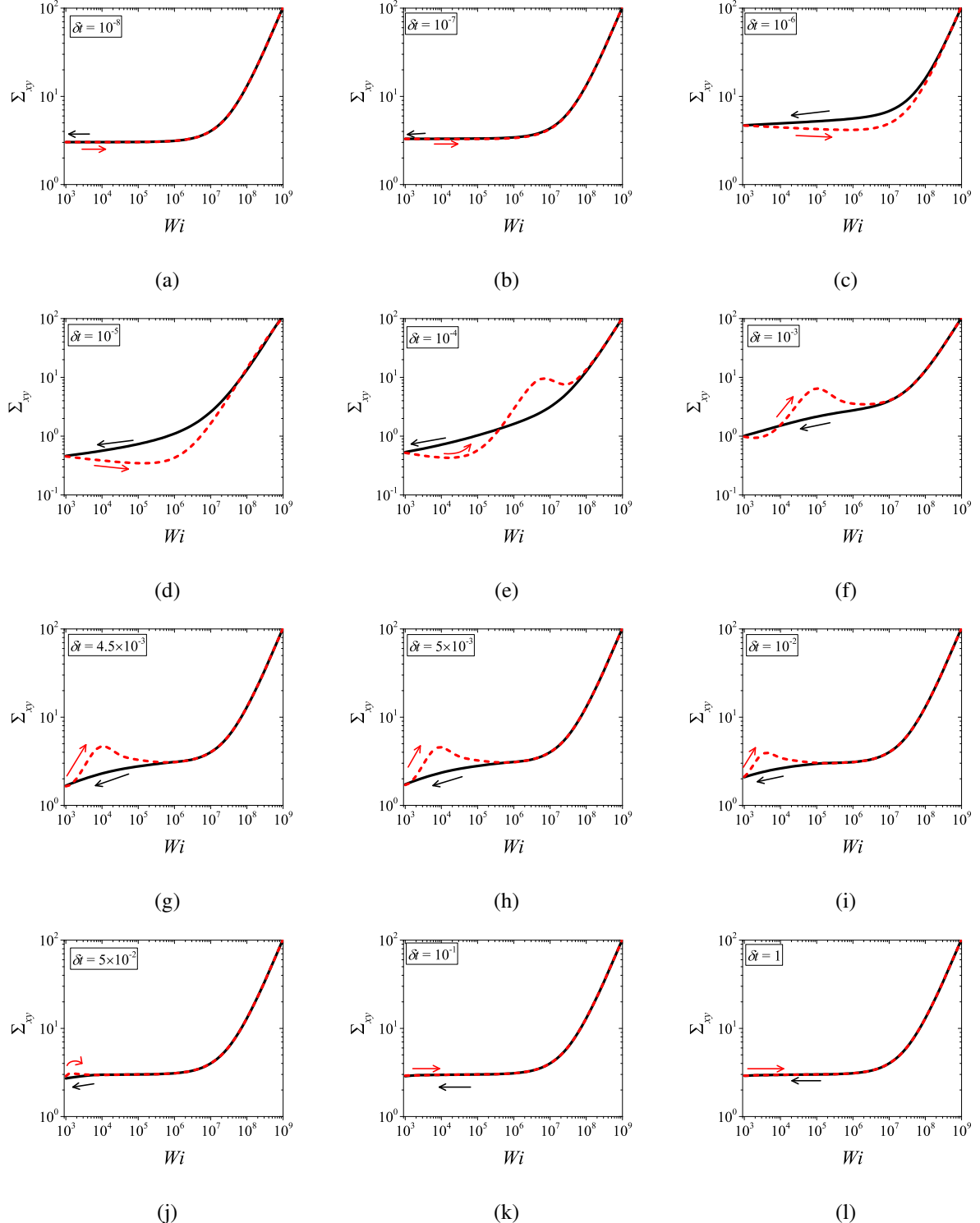


FIG. 3. Types of hysteresis loops (in a down-up shear rate cycle) obtained for the high relaxation time viscoelastic material using different values of δt and $\eta_s = 10^{-7}$. Shear stress is plotted as a function of shear rate (Wi) for δt (a) 10^{-8} , (b) 10^{-7} , (c) 10^{-6} , (d) 10^{-5} , (e) 10^{-4} , (f) 10^{-3} , (g) 4.5×10^{-3} , (h) 5×10^{-3} , (i) 10^{-2} , (j) 5×10^{-2} , (k) 10^{-1} , and (l) 1. Solid lines shows down-sweep and dashed line shows the up-sweep shear flow results.

3(i)). This is observed due to the fact that stress overshoot is triggered only in the shear-thinning part of the constitutive curve. In this case, type 5 loops can be obtained by linear viscoelastic effects, however, type 6 and 7 loops can only be obtained due to non-linear viscoelastic effects.

C. Area of hysteresis loop

In addition to the qualitative characteristics, hysteresis loops have also been characterised quantitatively using area of hysteresis loop in the literature. The area of hysteresis loop is obtained as mentioned in section II and is represented as A_σ . The plot of A_σ as a function of δt showed a bell-shaped curve for thixotropic materials and models [37, 40, and 43]. In these studies, the plot of A_σ as a function of δt showed a monotonic decrease of A_σ with δt for simple yield stress materials and models. The presence of bell-shaped curve in this plot has been treated as a signature of thixotropic nature of these materials and the value of δt corresponding to the peak in the bell-shaped curve is related to thixotropic time-scale of the material. In this subsection, we study the area of hysteresis loop obtained using a non-thixotropic viscoelastic model during the down-sweep and up-sweep shear flow. We measure the variation of area of hysteresis loop as a function of δt and also plot the loop area that is normalised with the area under the down-sweep curve (A_d). We show results for four cases (i) $\eta_s = 10^{-3}$, and Wi is varying from 10^{-5} to 10^{-1} in Fig. 4(a), (ii) $\eta_s = 10^{-3}$, and Wi is varying from 10^{-4} to 10^2 , in Fig. 4(b), (iii) $\eta_s = 10^{-7}$, and Wi is varying from 10^{-3} to 10^3 , in Fig. 4(c), and (iv) $\eta_s = 10^{-7}$, and Wi is varying from 10^3 to 10^9 , in Fig. 4(d). We find that loop area shows bimodal dependence for (ii), (iii), and (iv), and bell shaped dependence for (i). In all four cases, the loop area tends to zero if δt is significantly low. As explained above, this is due to no change in stress during down-sweep and up-sweep because of insufficient time of shearing at each step. The first increase in area as a function of δt in all four cases is due to incomplete stress relaxation decrease at the end of down-sweep, that continues in up-sweep and drives the up-sweep stress away from down-sweep stress. The incomplete decrease in stress during down-sweep continues to increase the loop area until the up-sweep stress shows a significant increase by getting more time of shearing in up-sweep which results in decreasing the loop area. These three processes lead to bell shaped curve in (i). The presence of stress overshoot in the up-sweep causes second increase in the loop area and its absence on increasing δt causes its final decay. The addition of second peak results into a bi-modal distribution of loop area when plotted against δt .

We also find that the second peak of (A_σ) is less significant for case (ii) and more significant for case (iii) and case (iv). This is due to two reasons, one is decrease in η_s value which causes amplification of underlying viscoelastic effects (these effects might get diminished at high Wi if η_s value is also high), and second is high value of Wi that results in more prominent overshoot in stress. The variation of A_σ/A_d in (ii), (iii) and (iv) show that the first peak of bi-modal graph is lower and the second peak is higher. In case (ii), the order of height of first and second peak of bi-modal graph is completely opposite to the order of first and second peak of A_σ bi-modal graph. This is due to the fact that for small values of δt , the change in down-sweep stress is minimal as shown in Fig. 2 which results in significantly high value of A_d for low values of δt and changes the height of first and second peak. In cases (iii) and (iv), A_σ/A_d is qualitatively similar to A_σ plot as A_d remains almost same for small values of δt (corresponding to first peak of A_σ/A_d plot). The value of A_d decreases for intermediate values of δt causing the amplification of second peak of A_σ/A_d plot.

The bell-shaped/bi-modal dependence of A_σ and A_σ/A_d on δt using a non-thixotropic viscoelastic model is qualitatively similar to that obtained using a thixotropic material and models in literature [37, 38, 40, and 43]. Furthermore, we find out the effect of number of steps taken per decade (n) and plot (A_σ) as a function of $n\delta t$ in Fig. 5. This plot also shows a bi-modal master curve which is independent of the value of n as shown in Fig. 5. This result is corresponding to results presented in Fig. 4(b). This master curve can be compared with the master curve of the thixotropic material obtained experimentally and by simulations [37, 40, and 43]. This result shows the underlying similarity in successfully getting a master curve using a non-thixotropic viscoelastic model and results of thixotropic models and materials reported in literature. Therefore, a master curve of (A_σ) as a function of $n\delta t$ also does not guarantee the identification of thixotropic and viscoelastic material. This result also shows that a bi-modal curve is independent of the type of flow protocol used to study hysteresis. For example, a combination of extremely high value of n and a very small value of δt can show results for continuous ramp down and ramp up flow.

D. Analysis

Figures 1-5 clearly state that the presence of (i) hysteresis loop, and (ii) bell-shaped/bi-modal dependence of A_σ on δt doesn't guarantee a material to be thixotropic. In this subsection, we analyze these two aspects in further details and discuss implications of the same.

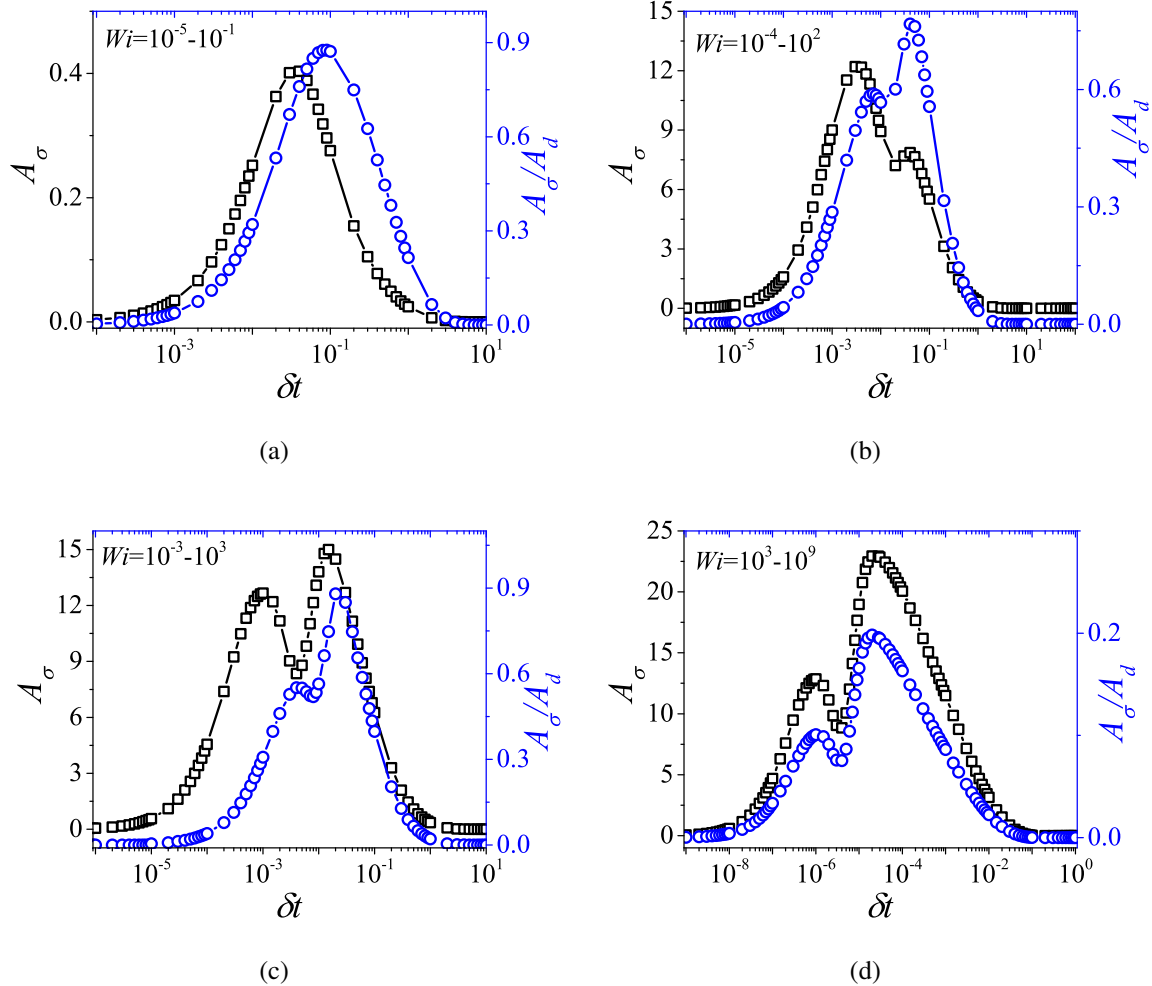


FIG. 4. Variation of area of hysteresis loop (A_σ) (on left y-axis) and normalised area of hysteresis loop (A_σ/A_d) (on right y-axis) is plotted with respect to δt . (a) A_σ is calculated for Wi varying in the range $10^{-5} - 10^{-1}$ for $n = 10$, $\eta_s = 10^{-3}$. (b) Wi is varying in the range $10^{-4} - 10^2$ for $n = 10$, $\eta_s = 10^{-3}$ and A_σ is calculated corresponding to the results plotted in Fig. 2. (c) A_σ is calculated for Wi varying in the range $10^{-3} - 10^3$ for $n = 10$, $\eta_s = 10^{-7}$. (d) Wi is varying in the range $10^5 - 10^9$ for $n = 10$, $\eta_s = 10^{-7}$ and area is calculated corresponding to the results plotted in Fig. 3. In Fig. (a), the hysteresis loops obtained are open for all the values of δt . In Fig. (c) hysteresis loops are open for $\delta t < 10^{-1}$. Square symbols shows A_σ and circle symbol shows A_σ/A_d and lines are guide to eyes in all the figures. In these figures, loop area shows a bi-modal curve which is qualitatively similar to bell shaped and bi-modal curve obtained using thixotropic materials in literature [37, 38, 40, and 43].

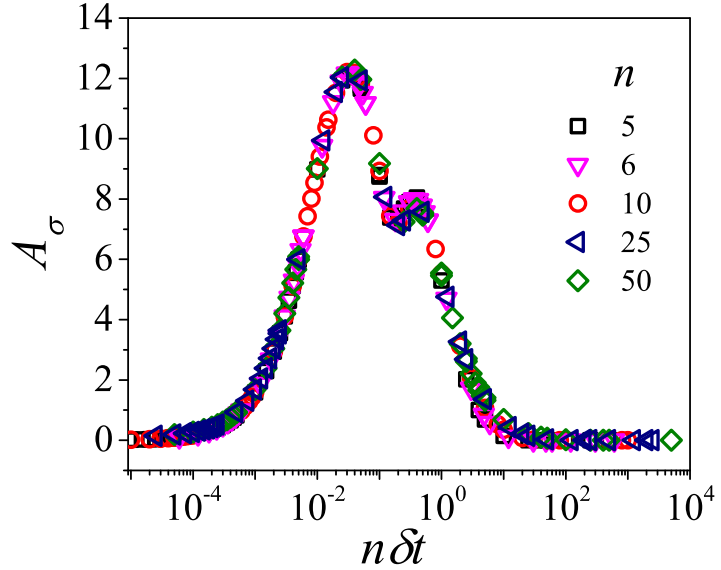


FIG. 5. Master curve of A_σ is plotted as a function of $n\delta t$ for different values of n . This result is obtained for Wi varying in the range $10^{-4} - 10^2$ and $\eta_s = 10^{-3}$.

1. Comparison of type of hysteresis loops

Radhakrishnan et al. [40] proposed the qualitative features of the hysteresis loops that are restricted only to a thixotropic material. They studied rheological hysteresis using a constitutive model and material that shows simple yield stress and viscoelastic bifurcation. The real materials were also viscoelastic in nature. Authors performed down-sweep followed by up-sweep shear rate experiments in a step-wise manner. Radhakrishnan et al. categorised hysteresis loops obtained using simple yield stress model with added viscoelasticity and viscosity bifurcating models (both models have a structure buildup term.). Authors mentioned that for a simple yield stress fluid with added viscoelasticity, stress during up-sweep shall be lesser (for the complete or some part of the range of shear rates) than stress during down-sweep shear flow. The authors also stated that a thixotropic material shall always show a stress higher in the up-sweep shear flow as compared to stress during down-sweep shear flow. This is due to a fact that a thixotropic material shows structure buildup at lower shear rate, and hence show a higher stress during up-sweep shear flow. The authors also explain that in the case of simple yield stress fluids, lower stress during up-sweep is due to the time taken by a material to reach the steady state because of added viscoelasticity. Stress during up-sweep may become higher than stress during down-sweep for a small range of

shear rates because of overshoot in shear stress.

We find that the hysteresis loop obtained for simple yield stress fluid with added viscoelasticity by Radhakrishnan et al. [40] is similar to loops obtained for a non-thixotropic viscoelastic model studied in the present work. Both the models also show open and closed hysteresis loops. The loops presented in Figs. 5 (a) and 5 (c) of their paper are similar to loops shown in Figs. 2(h)-2(j).

In addition to simple yield stress fluids, the hysteresis loops obtained for low relaxation time viscoelastic material also show similarity with hysteresis loops obtained for thixotropic materials. We mention here a few examples as follows. (i) Hysteresis loop obtained for waxy potato starch in paper by Krystyan et al. [17] is similar to the hysteresis loop in Figs. 2(h)-2(k) . (ii) Hysteresis loop of stress as a function of Mason number obtained using DPD simulation for an attractive colloidal particulate system by Jamali et. al. [43] in their Fig. 1(e) is similar to Figs. 2(j) and 2(k) of this study using a viscoelastic model.

However, the kind of hysteresis loops proposed by Radhakrishnan et al. [40] for thixotropic materials, wherein down-sweep stress is below the up-sweep stress is not observed for low relaxation time viscoelastic material. Nonetheless, these type of loops can be obtained using a high relaxation time viscoelastic material as shown in Figs. 3(g)-3(i). These loops are similar to many loops observed for thixotropic materials. A few examples are listed as follows. (i) Figure 2 (b) of Kurokawa et al. [36] using Ludox gel is similar to Figs. 3(e) and 3(f). (ii) Figure 8 (e) and 8 (f) of Fazilati et al. [18] using CNC suspension is similar to Fig. 3(g). (iii) Figure 8 of Divoux et al. [27] obtained using Carbopol microgel is similar to Figs. 3(g)-3(i). (iv) Figure 5(a) of Jamali and McKinley [38] obtained using structure kinetic model for a thixoviscous fluid is similar to Fig. 3(g)-3(i). Figure 6 shows a hysteresis loop in which shear stress is higher in the up-sweep shear flow than the stress during down-sweep shear flow for the complete range of Wi . This is obtained by varying Wi only for two decades i.e., $10^5 - 10^7$. Even though this type of loop is obtained by varying Wi for two decades, this plot is presented here only to show that a viscoelastic model is capable to show this type of loop. This loop is similar to Fig. 1(b) of Divoux et al. [37] obtained using Laponite dispersion.

The hysteresis loops presented in Figs. 1-3 and 6 covers all types of loops presented in literature for thixotropic materials. This similarity between the results of non-thixotropic viscoelastic model and thixotropic materials raises an important question as to whether it is possible to differentiate between a viscoelastic material and thixotropic material on the basis of hysteresis loops. Therefore, if a completely unknown material is to be identified as thixotropic or viscoelastic, then

rheological hysteresis may not be an ideal method to serve the purpose. This is because, as demonstrated in this study, just based on the hysteresis loop, the material could be a non-thixotropic viscoelastic material with a high relaxation time or it could be a thixotropic material as well.

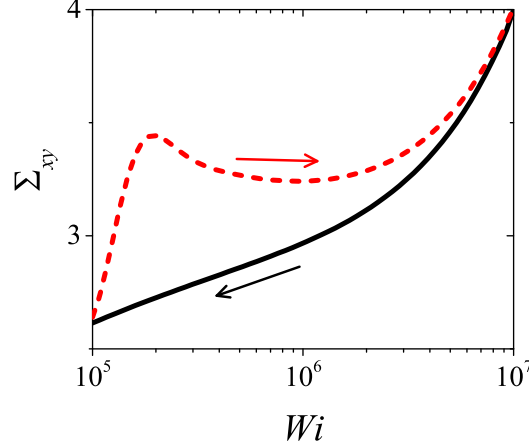


FIG. 6. Shear stress is plotted as a function of Wi for down-sweep and up-sweep shear flow by varying the Wi in the range of $10^5 - 10^7$. The value of η_s used to calculate this result is 10^{-7} . The down-sweep and up-sweep shear flow result for this case shows a hysteresis loop which is exactly similar to hysteresis loop observed for a thixotropic materials. Solid lines shows down-sweep and dashed line shows the up-sweep shear flow result.

2. Comparison of area of hysteresis loop

As mentioned above, the loop area has been reported to show a bell-shaped/bi-modal dependence for thixotropic materials in the literature [37, 38, 40, and 43]. We compare the bell-shaped/bi-modal dependence of thixotropic materials with bell-shaped/bi-modal dependence of non-thixotropic viscoelastic model. We find that the first peak of bi-modal dependence of A_σ/A_d is observed for very low values of δt which might not be realisable experimentally. Therefore, one may end up getting only the second peak in A_σ/A_d that is observed due to stress overshoot. For example, in case (iv) if $\tau = 10^5$ s, the first peak is observed for $\delta t \approx 10^{-6}$, which is around 0.1s of shearing time at each step. Most of the experimental studies use shearing time in the range $1 - 10^3$ s as also studied by Divoux et al. [37]. In this case, only second peak can be obtained for a viscoelastic fluid with very high relaxation time which also may erroneously identify a material as thixotropic.

Many studies also employ characteristic features of hysteresis loop to obtain thixotropic timescale. In various studies [37, 38, 40, 43, and 51] the thixotropic timescale (or characteristic timescale) is related to the value of δt corresponding to the peak in the $A_\sigma - \delta t$ plot as this plot has been reported to show a bell-shaped type for thixotropic materials. This technique assumes increase and decrease of A_σ is essentially due to thixotropy in the material. In the present work, we clearly show that viscoelasticity solely by itself, leads to a bell-shaped/bi-modal $A_\sigma - \delta t$ plot. In addition, very importantly, most of the tangible thixotropic materials are not inelastic, and have a finite non-zero relaxation time (in reality high relaxation time), and hence are strongly viscoelastic. Therefore, if the relaxation time is significantly high in a thixotropic material, which is usually the case, then there may be a case that peak will get shifted due to viscoelastic effects. As a result, quantification of thixotropic timescale using hysteresis loop method will always have a contribution from viscoelastic nature of a material. This contamination of viscoelasticity into thixotropic timescale may, therefore, lead to misleading or even erroneous results. Hence, hysteresis loop method may not be used to determine thixotropic timescale as well as any other thixotropic feature of the material if a material is also viscoelastic. Based on our results depicted in Fig. 2-6, an area enclosed by a hysteresis loop strongly depends on values of δt and the minimum and maximum value of Wi . In real viscoelastic materials, with large relaxation time and broad relaxation time distribution, the hysteresis is, therefore expected to be significant over a wide range of Wi and δt . Consequently, in a thixotropic material with broad viscoelastic relaxation time distribution, utmost care needs to be exercised while quantifying any thixotropic attributes of the same.

E. Viscoelastic hysteresis and shear banding

As mentioned in the Introduction, the rheological hysteresis has been linked with shear banding in the literature for thixotropic systems [37 and 40]. Divoux et al. [37] performed experiments on aqueous solution of Laponite with different concentrations and showed the presence of shear banding during up-sweep shear flow because of stress overshoot. The authors also showed the same for 1 wt. % aqueous solution of Carbopol. Radhakrishnan et al. [40] showed the presence of shear banding using structure kinetic model for simple yield stress fluids and viscosity bifurcating fluids. However, Puisto et. al. [39] showed that the presence of shear banding is only associated with a small range of shear rate in the up-sweep shear flow. Jamali et al. [43] noted that rheological hysteresis is more closely related to microstructure level dynamics than the flow heterogeneity or

mescoscale dynamics.

The above discussion is focused on the correlation between hysteresis and shear banding in thixotropic and simple yield stress fluids. However, in this work we have studied hysteresis using a non-linear viscoelastic model. In our recent study [52], we have proposed that stress overshoot does not necessarily lead to transient shear banding in a viscoelastic material using Johnson-Segalman, non-stretching Rolie-Poly, and the Giesekus model. Non-linear simulation results [53] also showed that stress overshoot does not lead to transient shear banding for Giesekus model. We, therefore, suggest that there may not be any correlation between viscoelastic hysteresis and shear banding in a viscoelastic material. This statement is applicable only if the underlying constitutive curve of the material is monotonic.

IV. CONCLUSIONS

In this work, we have studied rheological hysteresis using nonlinear viscoelastic model. We have followed the recently suggested protocol by Divoux et al. [37] wherein shear rate is varied in a step-wise manner from a high value to a low value (down-sweep) followed by a step-wise increase (up-sweep) to the original high value. We model the behaviour of two kinds of materials using Giesekus model, which is a standard nonlinear viscoelastic constitutive equation - those with low relaxation time $O(0.1$ s) and high relaxation time $O(10^6$ s) over a domain of realistic shear rates available in conventional rheometers (10^{-3} - 10^3 s $^{-1}$). We observe that both the kind of systems show pronounced hysteresis for practically explorable intermediate step time δt , with diminishing area enclosed by loop at high and low values of δt . This observation leads to a bell shaped or bimodal curve of area enclosed by hysteresis loop when plotted as a function of δt . The increasing part of the bell-shaped curve is due to incomplete stress relaxation during down-sweep shear flow. On the other hand, the decreasing part of the bell-shaped curve is because of up-sweep stress approaching its steady state value corresponding to each shear rate. The second peak in the bi-modal distribution curve, when observed, is because of stress overshoot during up-sweep shear flow. It is observed that the bell-shaped curve is obtained when the shear rate domain is in the linear viscoelastic region while the non-linear viscoelastic effects lead to bi-modal shaped curve. The hysteresis loops observed in the case of low relaxation time viscoelastic material can be open and closed but the hysteresis loops obtained using a high relaxation time viscoelastic materials are observed to be closed for all the values of δt .

Thixotropic materials also show a hysteresis loop for the mentioned flow protocol. In the literature, characteristics of a hysteresis loop are often employed to analyse behavior of thixotropic materials. Thixotropic materials also show a bell shaped when area enclosed by hysteresis loop is plotted against δt . Interestingly, the present work clearly shows that a viscoelastic material shows all the features of hysteresis that are usually attributed to the thixotropic materials. It is known that various real thixotropic materials employed in the literature have finite relaxation time and hence are also viscoelastic. Consequently, the present work suggests that while characterizing the hysteresis loop for a so-called thixotropic material, caution needs to be exercised in order to avoid contamination of viscoelastic effects to the hysteresis. We also note that while in some cases rheological hysteresis in thixotropic materials is also associated with a transient shear banding instability, rheological hysteresis in a viscoelastic material may not have any correlation with the transient shear banding instability if the underlying constitutive curve is monotonic.

ACKNOWLEDGMENT

We acknowledge financial support from the Science and Engineering Research Board, Government of India.

REFERENCES

- ¹H. A. Barnes, “Thixotropy—a review,” *Journal of Non-Newtonian fluid mechanics* **70**, 1–33 (1997).
- ²J. Mewis and N. J. Wagner, “Thixotropy,” *Advances in colloid and interface science* **147**, 214–227 (2009).
- ³R. G. Larson and Y. Wei, “A review of thixotropy and its rheological modeling,” *Journal of Rheology* **63**, 477–501 (2019).
- ⁴M. Agarwal, S. Sharma, V. Shankar, and Y. M. Joshi, “Distinguishing thixotropy from viscoelasticity,” *Journal of Rheology* **65**, 663–680 (2021).
- ⁵R. B. Bird and B. D. Marsh, “Viscoelastic hysteresis. part i. model predictions,” *Transactions of the Society of Rheology* **12**, 479–488 (1968).
- ⁶B. D. Marsh, “Viscoelastic hysteresis. part ii. numerical and experimental examples,” *Transactions of the Society of Rheology* **12**, 489–510 (1968).

⁷R. B. Bird and P. J. Carreau, “A nonlinear viscoelastic model for polymer solutions and melts—i,” *Chemical Engineering Science* **23**, 427–434 (1968).

⁸J. Greener and R. Connelly, “The response of viscoelastic liquids to complex strain histories: the thixotropic loop,” *Journal of Rheology* **30**, 285–300 (1986).

⁹F. Rubio-Hernández and A. Gómez-Merino, “Time dependent mechanical behavior: the viscoelastic loop,” *Mechanics of Time-Dependent Materials* **12**, 357–364 (2008).

¹⁰R. Larson, “Constitutive equations for thixotropic fluids,” *Journal of Rheology* **59**, 595–611 (2015).

¹¹J. Mewis, “Thixotropy—a general review,” *Journal of Non-Newtonian Fluid Mechanics* **6**, 1–20 (1979).

¹²A. Mujumdar, A. N. Beris, and A. B. Metzner, “Transient phenomena in thixotropic systems,” *Journal of Non-Newtonian Fluid Mechanics* **102**, 157–178 (2002).

¹³E. L. McMillen, “Thixotropy and plasticity. iii—the effect of thixotropy upon plasticity measurements,” *Journal of Rheology (1929-1932)* **3**, 179–195 (1932).

¹⁴R. Weltmann, “Thixotropic behavior of oils,” *Industrial & Engineering Chemistry Analytical Edition* **15**, 424–429 (1943).

¹⁵S. J. Hahn, T. Ree, and H. Eyring, “Flow mechanism of thixotropic substances,” *Industrial & Engineering Chemistry* **51**, 856–857 (1959).

¹⁶H. Green, “High-speed rotational viscometer of wide range. confirmation of thereiner equation of flow,” *Industrial & Engineering Chemistry Analytical Edition* **14**, 576–585 (1942).

¹⁷M. Krystyjan, M. Sikora, G. Adamczyk, A. Dobosz, P. Tomaszik, W. Berski, M. Łukasiewicz, and P. Izak, “Thixotropic properties of waxy potato starch depending on the degree of the granules pasting,” *Carbohydrate polymers* **141**, 126–134 (2016).

¹⁸M. Fazilati, S. Ingelsten, S. Wojno, T. Nypelö, and R. Kádár, “Thixotropy of cellulose nanocrystall suspensions,” *Journal of Rheology* **65**, 1035–1052 (2021).

¹⁹S. W. Jeong, J. Locat, J. K. Torrance, and S. Leroueil, “Thixotropic and anti-thixotropic behaviors of fine-grained soils in various flocculated systems,” *Engineering Geology* **196**, 119–125 (2015).

²⁰D. Perret, J. Locat, and P. Martignoni, “Thixotropic behavior during shear of a fine-grained mud from eastern canada,” *Engineering Geology* **43**, 31–44 (1996).

²¹M. Fourmentin, G. Ovarlez, P. Faure, U. Peter, D. Lesueur, D. Daviller, and P. Coussot, “Rheology of lime paste—a comparison with cement paste,” *Rheologica Acta* **54**, 647–656 (2015).

²²J. Ma, Y. Lin, X. Chen, B. Zhao, and J. Zhang, “Flow behavior, thixotropy and dynamical viscoelasticity of sodium alginate aqueous solutions,” *Food Hydrocolloids* **38**, 119–128 (2014).

²³R. Durairaj, N. Ekere, and B. Salam, “Thixotropy flow behaviour of solder and conductive adhesive pastes,” *Journal of materials science: materials in electronics* **15**, 677–683 (2004).

²⁴Z. Li, D. Li, Y. Chen, and H. Cui, “Study of the thixotropic behaviors of ferrofluids,” *Soft matter* **14**, 3858–3869 (2018).

²⁵M. V. Ghica, M. Hîrjău, D. Lupuleasa, and C.-E. Dinu-Pîrvu, “Flow and thixotropic parameters for rheological characterization of hydrogels,” *Molecules* **21**, 786 (2016).

²⁶C. Wang, L. Qiu, and T. Wang, “Self-assembly and rheological behaviors of intermacromolecular complexes consisting of oppositely charged fluorinated guar gums,” *Carbohydrate polymers* **184**, 333–341 (2018).

²⁷T. Divoux, C. Barentin, and S. Manneville, “From stress-induced fluidization processes to herschel-bulkley behaviour in simple yield stress fluids,” *Soft Matter* **7**, 8409–8418 (2011).

²⁸M. Iotti, Ø. W. Gregersen, S. Moe, and M. Lenes, “Rheological studies of microfibrillar cellulose water dispersions,” *Journal of Polymers and the Environment* **19**, 137–145 (2011).

²⁹J. Labanda and J. Llorens, “Influence of sodium polyacrylate on the rheology of aqueous laponite dispersions,” *Journal of colloid and interface science* **289**, 86–93 (2005).

³⁰L. Chen, C. Zukoski, B. Ackerson, H. Hanley, G. Straty, J. Barker, and C. Glinka, “Structural changes and orientaional order in a sheared colloidal suspension,” *Physical review letters* **69**, 688 (1992).

³¹R. Mendes, G. Vinay, G. Ovarlez, and P. Coussot, “Reversible and irreversible deconstructing flow in waxy oils: An mri study,” *Journal of Non-Newtonian Fluid Mechanics* **220**, 77–86 (2015).

³²B. Baldewa and Y. M. Joshi, “Thixotropy and physical aging in acrylic emulsion paint,” *Polymer Engineering & Science* **51**, 2085–2092 (2011).

³³B. Derakhshandeh, D. Vlassopoulos, and S. G. Hatzikiriakos, “Thixotropy, yielding and ultrasonic doppler velocimetry in pulp fibre suspensions,” *Rheologica acta* **51**, 201–214 (2012).

³⁴W. M. Holmes, P. T. Callaghan, D. Vlassopoulos, and J. Roovers, “Shear banding phenomena in ultrasoft colloidal glasses,” *Journal Of Rheology* **48**, 1085–1102 (2004).

³⁵F. Da Cruz, F. Chevoir, D. Bonn, and P. Coussot, “Viscosity bifurcation in granular materials, foams, and emulsions,” *Physical Review E* **66**, 051305 (2002).

³⁶A. Kurokawa, V. Vidal, K. Kurita, T. Divoux, and S. Manneville, “Avalanche-like fluidization of a non-brownian particle gel,” *Soft Matter* **11**, 9026–9037 (2015).

³⁷T. Divoux, V. Grenard, and S. Manneville, “Rheological hysteresis in soft glassy materials,” *Physical review letters* **110**, 018304 (2013).

³⁸S. Jamali and G. H. McKinley, “The mnemosyne number and the rheology of remembrance,” *arXiv:2201.01201*.

³⁹A. Puisto, M. Mohtaschemi, M. J. Alava, and X. Illa, “Dynamic hysteresis in the rheology of complex fluids,” *Physical Review E* **91**, 042314 (2015).

⁴⁰R. Radhakrishnan, T. Divoux, S. Manneville, and S. M. Fielding, “Understanding rheological hysteresis in soft glassy materials,” *Soft Matter* **13**, 1834–1852 (2017).

⁴¹P. Sollich, F. Lequeux, P. Hébraud, and M. E. Cates, “Rheology of soft glassy materials,” *Physical review letters* **78**, 2020 (1997).

⁴²P. Sollich, “Rheological constitutive equation for a model of soft glassy materials,” *Physical Review E* **58**, 738 (1998).

⁴³S. Jamali, R. C. Armstrong, and G. H. McKinley, “Multiscale nature of thixotropy and rheological hysteresis in attractive colloidal suspensions under shear,” *Physical review letters* **123**, 248003 (2019).

⁴⁴H. Giesekus, “A simple constitutive equation for polymer fluids based on the concept of deformation-dependent tensorial mobility,” *Journal of Non-Newtonian Fluid Mechanics* **11**, 69–109 (1982).

⁴⁵M. E. Helgeson, M. D. Reichert, Y. T. Hu, and N. J. Wagner, “Relating shear banding, structure, and phase behavior in wormlike micellar solutions,” *Soft Matter* **5**, 3858–3869 (2009).

⁴⁶A. S. Khair, “Large amplitude oscillatory shear of the giesekus model,” *Journal of Rheology* **60**, 257–266 (2016).

⁴⁷D. Vlassopoulos and S. G. Hatzikiriakos, “A generalized giesekus constitutive model with retardation time and its association to the spurt effect,” *Journal of non-newtonian fluid mechanics* **57**, 119–136 (1995).

⁴⁸E. Menezes and W. Graessley, “Nonlinear rheological behavior of polymer systems for several shear-flow histories,” *Journal of Polymer Science: Polymer Physics Edition* **20**, 1817–1833 (1982).

⁴⁹J. M. Dealy and K. F. Wissbrun, “Transient shear flows used to study nonlinear viscoelasticity,” in Melt Rheology and Its Role in Plastics Processing (Springer, 1999) pp. 179–230.

⁵⁰R. I. Tanner, Engineering rheology, Vol. 52 (OUP Oxford, 2000).

⁵¹E. Javadi and S. Jamali, “Thixotropy and rheological hysteresis in blood flow,” *The Journal of Chemical Physics* (2022).

⁵²S. Sharma, V. Shankar, and Y. M. Joshi, “Onset of transient shear banding in viscoelastic shear start-up flows: Implications from linearized dynamics,” *Journal of Rheology* **65**, 1391–1412 (2021).

⁵³R. L. Moorcroft and S. M. Fielding, “Shear banding in time-dependent flows of polymers and wormlike micelles,” *Journal of Rheology* **58**, 103–147 (2014).